AIAA Flight Testing Conference, AIAA AVIATION Forum,
5-9 June 2017, Denver, Colorado, USA.
(AIAA 2017-3652)

Aircraft spin analysis - theoretical predictions & comparison to flight test

Christopher Bennett* and Nicholas Lawson†

National Flying Laboratory Centre, School of Aerospace, Transport and Manufacturing, Cranfield University, UK.

A Scottish Aviation Bulldog light aircraft operated by the National Flying Laboratory Centre (NFLC) at Cranfield University, modified with research equipment including fibre optic sensors for wing strain and fuselage pressure measurements, is used to investigate the dynamics of a fully developed spin. A theoretical model is developed to compare with existing flight test data. In particular, the frequency of the aircraft spin is analysed as a function of the mass distribution of the aircraft to determine the effect of the fuel load.

It is found that the spin frequency is minimally affected by the fuel load since the moments of inertia corresponding to the engine, for example, are far more significant. However, it is confirmed that the yawing effect of the propeller causes the aircraft to spin faster to the right than to the left.

I. Introduction

A spin is defined as an auto-rotating decent of a stalled aircraft in a helical pattern about the vertical axis. The situation occurs when the critical angle of attack is exceeded, leading to flow separation on the upper surface of the wings and a reduction in lift. Under adequate side-slip and yaw rates, an imbalance of load on the wings during stall conditions causes one wing to drop and hence the initiation of a spin, often referred to as the incipient stage. The spin quickly stabilises into the fully developed stage, in turn leading to a rapid decent of the aircraft.

The spin is a dangerous scenario for pilots without adequate training, experience and skill. Aerobatic and utility category aircraft are certified such that recovery from a spin is achievable, and so pilots of these categories of aircraft are trained in recovering from spins. Despite this, the majority of the literature regarding the aircraft spin is focused on prevention and recovery from a safety or design point of view, rather than the aerodynamic features. Limited work has been completed on aircraft dynamics during the spin, particularly in the fully developed, stable stage. Very complex dynamics are apparent due to the number of factors which affect the frequency of the spin and path of the downward trajectory.

The most significant experimental and theoretical work in the field was conducted throughout the 1940's, 50's and 60's with emphasis on aircraft design and safety. During this period, the classic works on aircraft stability and control[1–3] discuss the general dynamics of the spin, either as a consequence of the stall, or in the context of aircraft tail section design to facilitate improved response to spin recovery techniques. Furthermore, extensive free flight model testing (as opposed to on a spinning rig) was carried out throughout the same period at NACA's 15 and 20-foot spin tunnel facilities at Langley Research Center in Hampton, Virginia, USA.[4] Results for an extensive array of aircraft, from jet fighters to large transport aircraft, are summarised in the NACA research memorandum.[4] Data was gathered for a range of aileron and elevator deflections and mass loading conditions for each aircraft, as well as photographs showing the spin trajectory. Analysis regarding the steady state and spin recovery characteristics of the aircraft was aimed at improvements in aircraft design, particularly for satisfactory spin recovery.

Since the publication of these early works, research in the area of spin dynamics appears to have received diminishing attention, meaning that the long established equations and methodology from these pioneering authors are widely accepted to the present day. The large number of factors affecting the dynamics of any

*Postdoctoral Research Fellow, National Flying Laboratory Centre.
†Professor in Aerodynamics and Airborne Measurement, National Flying Laboratory Centre.

given aircraft spin, and the requirement for flight testing, may be the reason for the stagnation in this area. However, in this paper, data collected from the newly developed Bulldog flight test bed, discussed in more detail in the following section, and the comparison to the established theory provides a novel insight into spin dynamics. A revised mathematical approach is aimed at theoretically predicting the frequency of a fully developed spin based on the mass distribution of a Bulldog light aerobatic aircraft in configurations with high and low fuel loads. The calculations will show that the moments of inertia corresponding to the fuel load is insignificant in comparison to the larger masses such as the engine. This finding will be confirmed through airborne test data obtained previously[5,6] from inertial and fibre optic sensors, described in the next section, where it was seen that the spin frequency is minimally affected by the differences in fuel load.

II. Flight Test Set-up and Equipment

A Scottish Aviation Bulldog, operated by the National Flying Laboratory Centre at Cranfield University for research purposes, has undergone a number of modifications to transform it into a research test bed.[7] Fig. 1 shows the various sensors and systems fitted to the Bulldog.

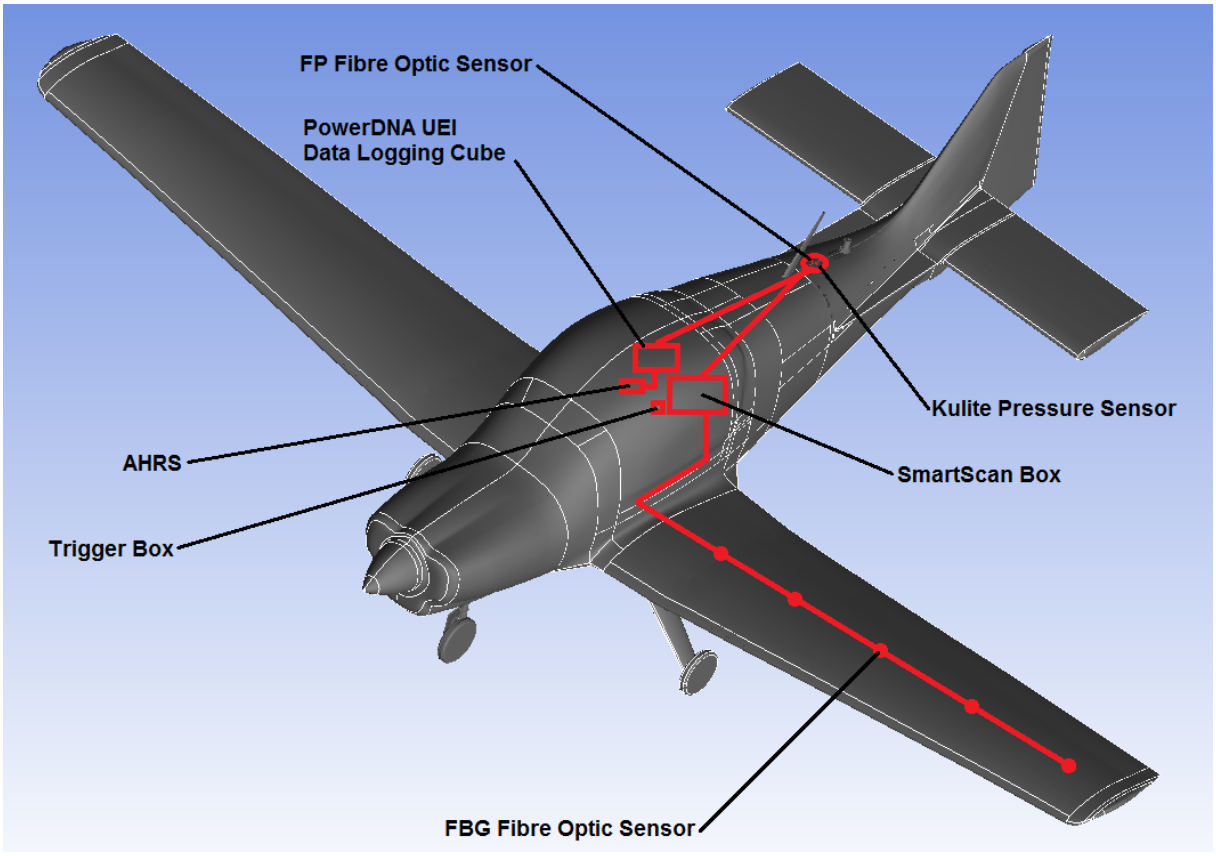

Figure 1. Diagram showing the sensors and systems on the Bulldog.

The first modifications with particular relevance to this study are the five Fibre Bragg Grating (FBG) sensors distributed along the main spar of the port side wing at distances $550mm$, $750mm$, $1550mm$, $2550mm$, and $2950mm$ from the side of the fuselage. Four of the FBGs record wing strain data while the fifth, floating inside a hypodermic tube, is used to temperature correct the other four sensors. This data is recorded by a SmartScan Aero interrogator box, located inside the cockpit with a sampling rate of 2 kHz.

Secondly, an SBG Systems IG-500A Attitude and Heading Reference System (AHRS), located close to the Bulldog's centre of gravity (C. G.) and positioned on the fuselage reference line connecting the tip of the spinner and the corner of the rudder, provides 3-dimensional attitude and acceleration data: pitch, roll and yaw rates. This data is used to correlate the fibre optic sensor data with specific dynamic and aerobatic

manoeuvres. The AHRS data is recorded by a PowerDNA UEI data logging cube located inside the cockpit.

All modifications to the Bulldog were completed as a minor modification under Certification Specification 23 (CS-23), with $13kg$ added to the total weight of the aircraft and a negligible change to the C. G. position. All sensors were ground and laboratory calibrated before flight tests were undertaken.[7]

III. Flight Test Methodology

The Bulldog research test bed described above was previously used to gather data for a range of aerobatic and high-g manoeuvres, including left- and right-hand spins.[5,7] Of interest here are the test flights where controlled spins were performed for a range of fuel loads.

The aircraft's fuel tanks are situated in the wings close to the leading edge. Fuel is filled from the outermost end of the wing and flows through a series of subsections of the tank, separated by non-return valves, to the most inboard area of the tank. This ensures that under centrifugal force, fuel is not forced outboard. As the fuel load does not shift laterally during a spin, it contributes minimally to the gyroscopic effect of the aircraft, and also prevents the engine from leaning out under such conditions. The aircraft's fuel load is therefore a convenient way of altering the mass distribution.

As recommended in the flight manual, all spins were performed with an approximately equal fuel load in each tank. Furthermore, a maximum of four spins per flight were performed with the direction of the spin alternating each time, with on average four to five turns per spin.

The data obtained from the fibre optic sensors, AHRS, and on-board video were re-processed and analysed for the purpose of this study. Flight test results for high fuel load cases will be used to predict spin characteristics for a low fuel load case via a revised theoretical model derived in the following section. The theoretical predictions will then be compared to low fuel load flight test results to examine the accuracy of the model.

IV. Flight Test Error Analysis

The first consideration is that of pilot error and repeatability. It is possible that the way in which the spin is induced characterises the spin entry phase, which can in turn affect the development of the spin at the stable stage. Clearly, without control position sensors it is not possible to quantify the pilot inputs which initiate the spin. Therefore, it will be assumed in this paper that pilot technique had negligible affect on the spin characteristics. Furthermore, it will be assumed that the controls for the aileron, rudder and engine settings are consistent for all the spins.

Table 1 lists the relevant errors of the on-board equipment used for the flight tests based on the laboratory calibration[7] and manufacturers data sheets,[8] and the sampling rates of the sensors are summarised in Table 2. A 95% confidence interval based on these errors is incorporated into the final results.

Variable	Accuracy
Fuel Quantity	$\pm$0.5L
AHRS (Dynamic Manoeuvre)	$\pm2^\circ$ RMS[8]
AHRS Repeatability	$\pm0.2^\circ$[8]
AHRS Resolution	$\pm0.05^\circ$[8]
FBG (Wing Strain)	$\pm0.5\mu m$[7]

Table 1. Summary of flight test data uncertainties and accuracies.

V. Features of the Spin and Mathematical Model

Referring to the literature,[1–3] features of the Bulldog spin can be identified theoretically for a range of angles of attack, α, by manipulating a number of key equations. During a spin, the aircraft's helical downward motion rotates around a vertical axis defined as the centre of rotation. The spin radius, R, is defined as the distance between the aircraft C. G. defining the flight path, and the centre of rotation, see

Variable	Sampling Frequency (Hz)
AHRS	100 (max)[8]
Fibre optic strain sensors	2500 (max)[7]
Fibre optic pressure sensor	2500 (max)[7]
Kulite	2500 (set)[5]

Table 2. Summary of flight test data sampling frequencies.

Fig. 2. With the aircraft oriented in a nose down attitude, α is defined as the angle between the downward helical flight path angle, γ, and the aircraft reference line.

In order to apply moment of inertia theory to find the difference in spin frequency, the distance between the aircraft's centre of gravity and centre of rotation must be found. Hence, the spin radius, R, is the key parameter to find via traditional theoretical methods. For reference, a number of parameters specific to the Bulldog and the spin flight conditions are listed in Table 3.

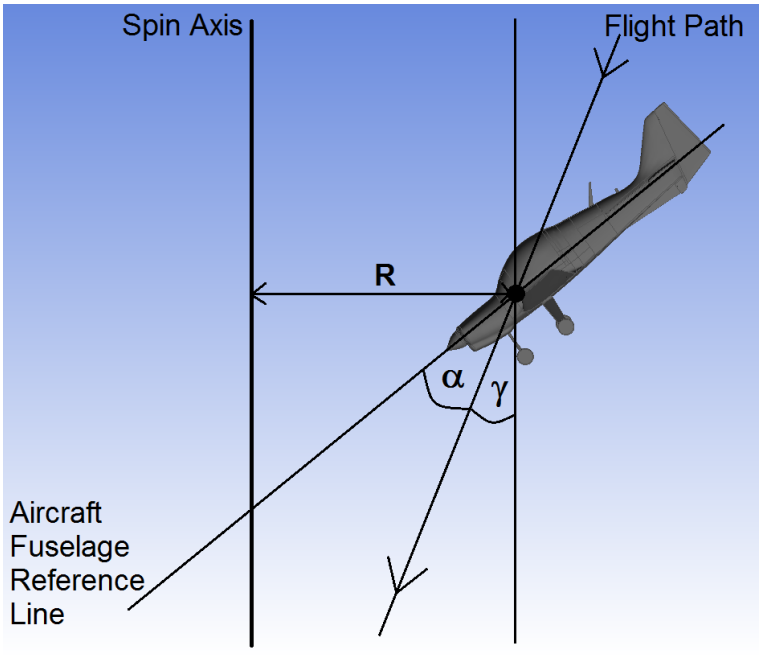

Figure 2. Diagram of the spin motion.

It is possible that during a spin, the effective angle of attack can be anywhere in the range 0-90°, where fast flat spins will have a characteristic angle of attack close to 90° and a slow steep spin will have a characteristic angle of attack close to 0°. Therefore, the aircraft's behaviour in extreme attitudes should be considered in the succeeding calculations for completeness of the model.

Firstly, the angle of attack, α, is related to the helical flight path angle, γ, via a linear relationship depicted in[2] Fig. 16.4 , which is extended to consider a full range of angles of attack from 0-90°. Next, the aircraft's lift and drag characteristics beyond the stall angle of attack are approximated based on general data for an aircraft with unswept rectangular wings.[9] The shape of the curve relating the lift coefficient to angle of attack can be approximated by a series of linear and quadratic sections. The function is modified for the specific case of the Bulldog to incorporate the corresponding maximum lift coefficient, as found in the flight test data,[6] and is also extended to an angle of attack of 90°. The drag coefficient can be approximated by a trigonometric function and extended to a maximum drag coefficient at 90° based on results for bluff bodies at comparable Reynolds numbers.[10] The key Bulldog lift and drag characteristics, up to near the stall point, can also be validated from previous flight test data.[6] The resulting curves, showing variation

Aerofoil	NACA - 63_2615
Wing reference area (m)	12.02
Wing Aspect Ratio	8.4
Zero Fuel Mass (kg)	885
Fuel Mass (kg)	60 - 130
Stall Speed (m/s)	27.7
Air density (kg/m^3)	0.9936
Accel due to gravity (m/s^2	9.8

Table 3. Bulldog reference values.

of C_L and C_D with angle of attack, are given in Fig. 3. Similar techniques to approximate lift and drag coefficients at high angles of attack have been utilized previously to consider insect flight[11] and helicopter blades.[12] The curves are comparable to NACA published data for the Bulldog's specific aerofoil for low to mid angles of attack, where the data ends, with an extension to higher angles of attack via a function similar to that given in the classical work by Hoerner and Borst.[13]

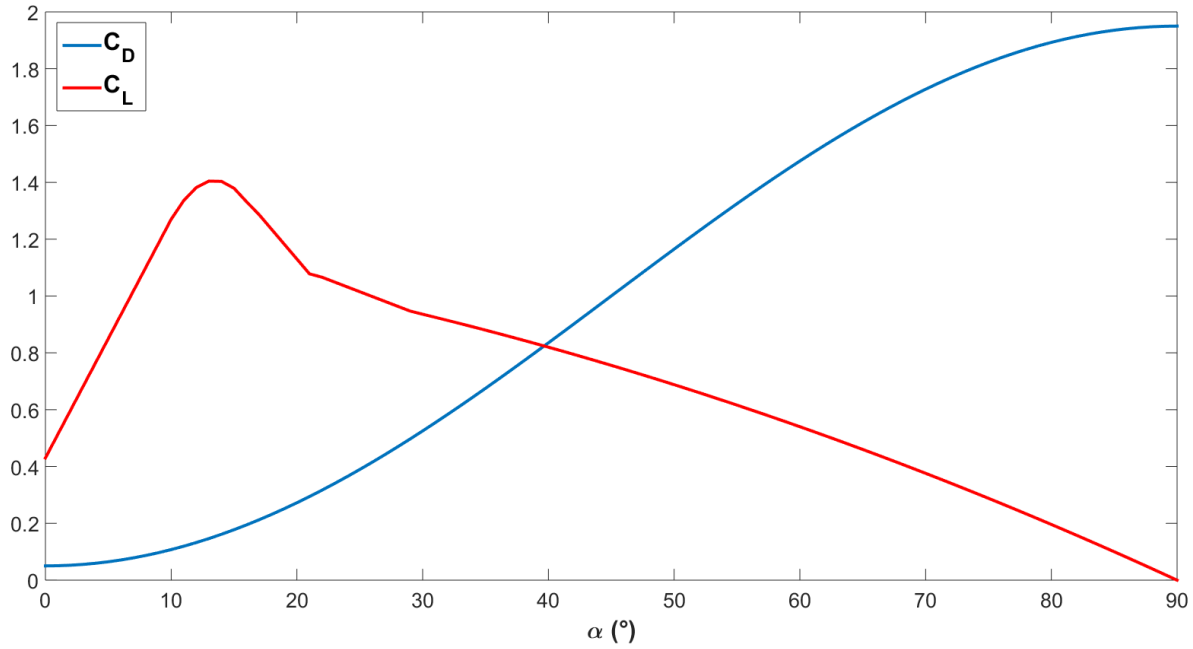

Figure 3. C_L and C_D characteristics for high angles of attack.

Now that the lift and drag coefficients are defined, the resultant force coefficient, C_R, can be found via

$$C_R = \sqrt{{C_D}^2 + {C_L}^2}. \tag{1}$$

Next, the rate of vertical decent, V_0, is calculated via the following equation given in Babister,[2] found from resolving horizontal and vertical forces on the aircraft

$$V_0^2 = \frac{2mg}{\rho S C_R \sin\alpha}, \tag{2}$$

where m is the total mass of the aircraft, g is the acceleration due to gravity, ρ is the air density, and S is

the wing reference area. Then, using the equation for the horizontally resolved forces,

$$mR\Omega^2 = \frac{1}{2}\rho V_0^2 S C_L, \tag{3}$$

and the equation for the flight path angle from the same publication

$$\tan\gamma = \frac{R\Omega}{V_0}, \tag{4}$$

the angular velocity of the spin, Ω, can be found by rearranging both equations (3) and (4) for R and equating, thus,

$$\Omega = \frac{\rho V_0 S C_L}{2m\tan\gamma}. \tag{5}$$

Finally, the radius of the spin, R, can now be found by substituting Ω into equation (4). Fig. 4 shows how the angle of attack affects the radius of the spin. Note that the jump discontinuity in the derivative of the function is a direct result of the adjoining C_L approximations. However, generally speaking, this result is consistent with the common observation that a flat spin is faster and of a much tighter radius than a steep spin.

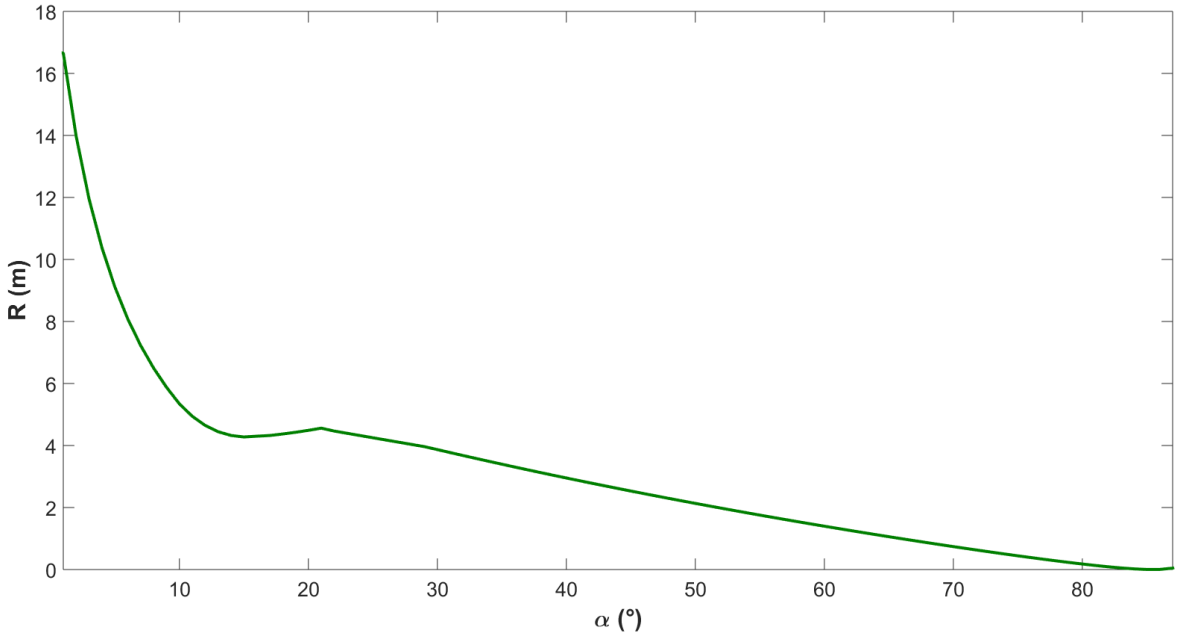

Figure 4. Variation of the spin radius depending on the angle of attack.

Having calculated the spin radius, it is possible to calculate the moments of inertia of the significant point masses which make up the total aircraft mass since the corresponding distances from the centre of rotation are now known. Step by step calculations are given in Section VII.

VI. High Fuel Load Flight Test Analysis

The high fuel load flight test is considered as a benchmark case. Features and characteristics of the various spins are analysed via the flight test equipment described in Section II. Four spins were performed in this particular flight test: two left and two right. AHRS and FBG fibre optic sensor data from this flight test is shown in Figs. 5 and 6. Note that high and low pass filters have been applied to the FBG data to avoid frequency spikes due to noise. The spin manoeuvres are clearly visible in both figures, and also the direction of the spin is easily identified from the angular rates shown in Fig. 5: positive angular rates correspond to spins to the right.

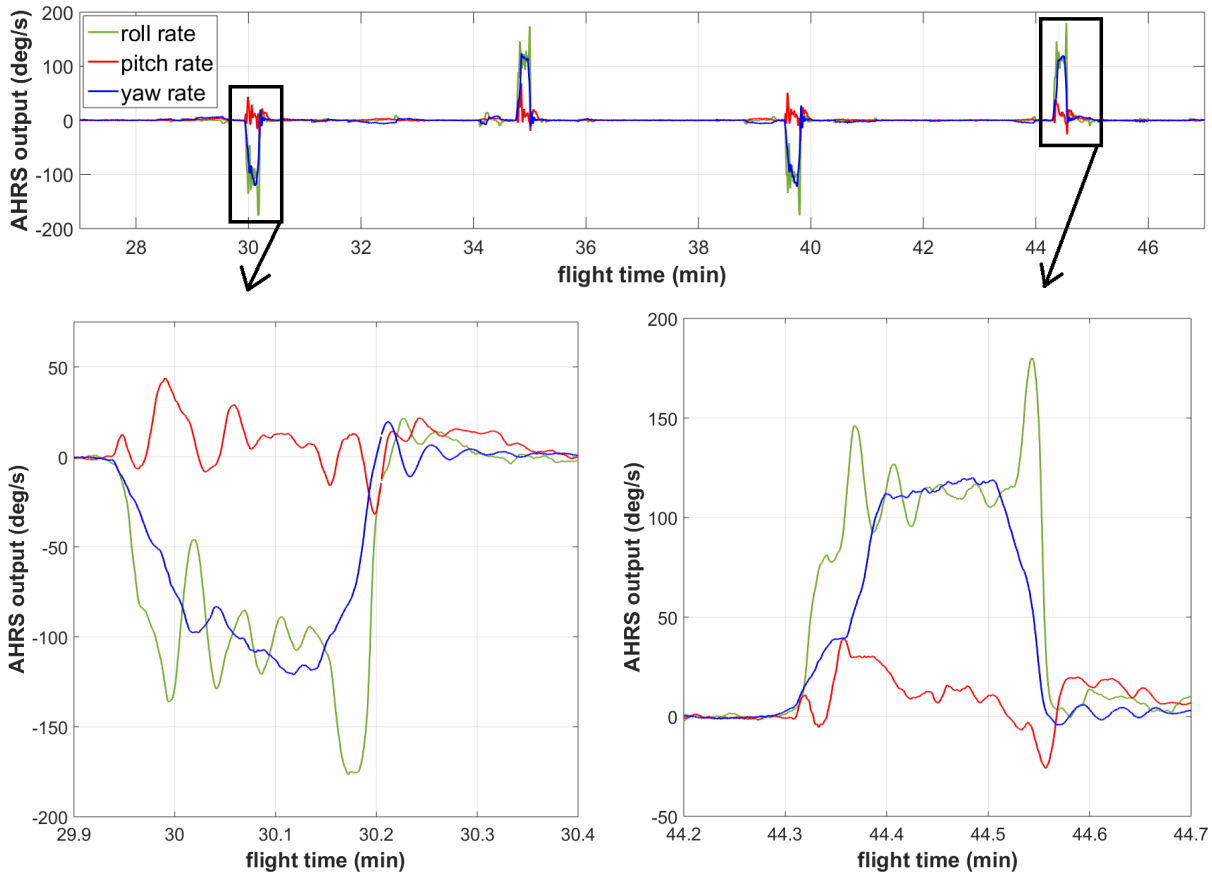

Figure 5. AHRS data for the high fuel load flight test showing the roll, pitch and yaw rates for 4 distinct spins. Overview of the flight test showing alternating spins to the left and right (upper), and zoomed-in views showing an example left and right spin (lower).

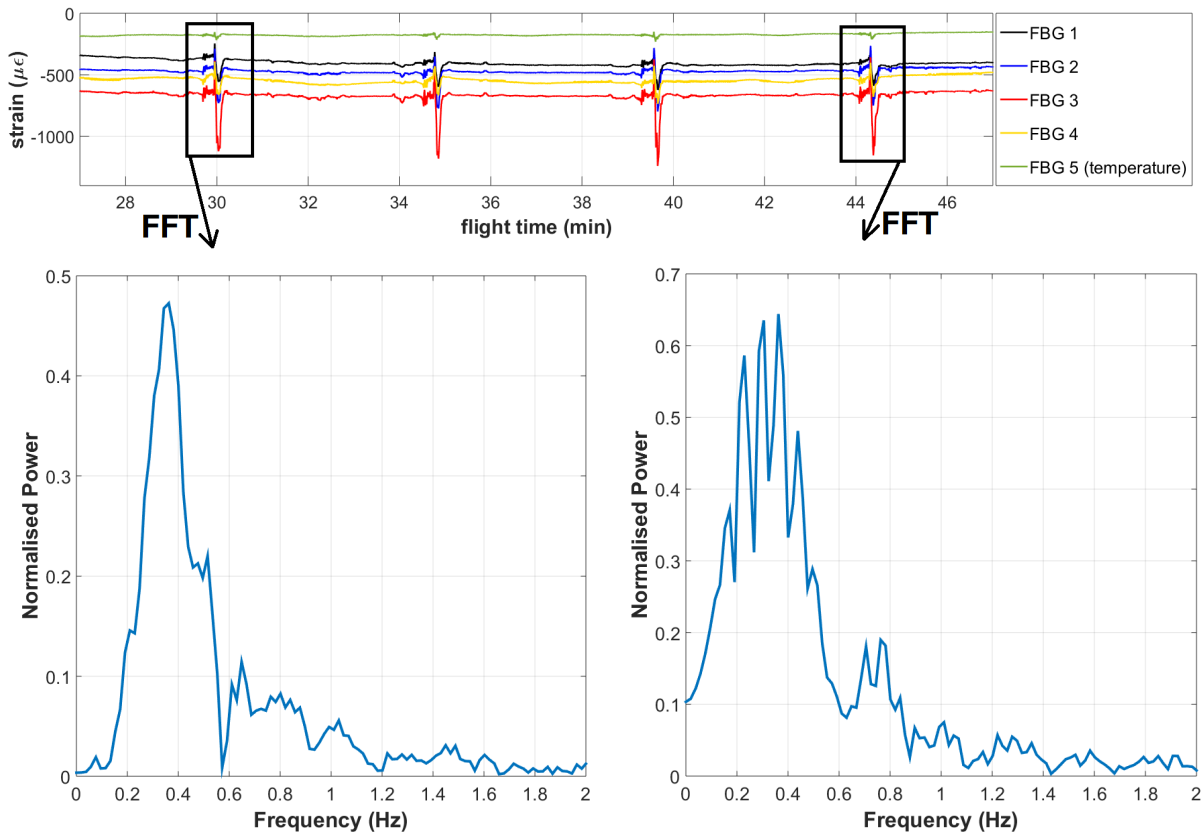

Figure 6. FBG data for the high fuel load flight test showing the 4 distinct spins. Overview of the flight test showing 4 spins (upper), and FFT plots showing the dominant frequency of an example left and right spin (lower).

The frequency of the developed spin is calculated using a combination of the AHRS and FBGs data. It is seen that during any given spin, the yaw rate stabilises once the spin reaches the fully developed stage, see Fig. 5. At this point, the spin frequency is calculated by taking 360° divided by the yaw rate. To confirm this result, the start and end points of a spin manoeuvre, determined from the AHRS data, are used to apply a Fast Fourier Transform (FFT) to the FBG data to find the dominant spin frequency for the stable stage, see Fig. 6. It is seen that both methods yield a similar result.

In addition to the frequencies, other characteristics of the spin can be determined from the data presented in Figs. 5 and 6. The AHRS pitch attitude data can be converted into angle of attack by subtracting the flight path angle. Fig. 7 shows the angle of attack variation for an example spin. It is assumed that the aircraft is in straight and level flight, and hence tracks a flight path angle of zero degrees, in the stall phase. At the point where the stall develops into a spin, it is assumed that the flight path angle changes instantaneously to a steep decent[a]. Therefore, the incipient stage of the spin is not fully captured in this region of the data and would be expected to be in the form of a more complex and continuous transition, without such a discontinuity. Similarly, in the recovery stage, the flight path angle is gradually restored to straight and level from a steep decent. Hence an approximate linear transition has been applied to the data for the recovery stage. Finally, a correction is applied to the pitch angle data as in[6] to account for the wing chord line offset, as compared to the fuselage reference line on which the AHRS is mounted.

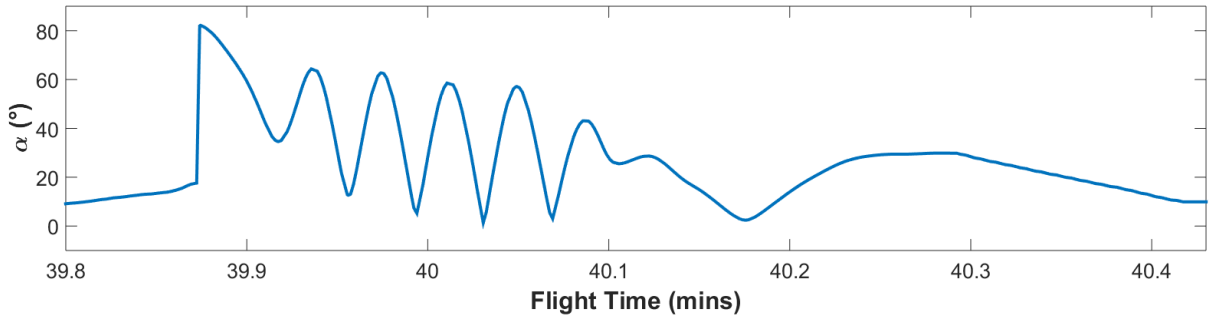

Figure 7. Angle of attack variation for an example spin manoeuvre taken from the high fuel load flight test.

The radius of the spin can therefore be determined by correlating the angle of attack data, such as that given in Fig. 7, with the spin radius function given in Fig. 4. Since the angle of attack oscillates throughout the spin, even in the fully developed stable stage, so does the spin radius. The range of angles of attack attained during the steady state spin corresponds to spin radii between 2 and 10 metres.

Further analysis of the high fuel load flight test data shows that the oscillations in pitch attitude, as shown in Fig. 7, corresponds approximately with the spin frequency. Therefore the aircraft C. G. actually tracks an ellipse around the centre of rotation, see Fig. 8 left. In the initial stages of the spin, an elongated elliptical path is traversed before decaying into a more circular orbit. However, if the pitch attitude oscillations and the rotational frequency are not in phase, for example in Fig. 8 right, where the pitch attitude oscillation is 25% greater than the rotational frequency, the aircraft's C. G. may potentially traverse an epicycloid pattern around the centre of rotation. Although the flight test results are accompanied with on board video, it is impossible to confirm this result without an external visualization of the spin, preferably from directly above or below. The non-circular spin trajectory may be a result of how the spin is initiated and/or propeller yawing and slipstream effects, commonly referred to as the P-factor, which differ between left- and right-hand spins.

Therefore, to allow comparison of the flight test results to the theory, in the following section an average angle of attack will be taken for the fully developed stage of the spin. This will allow an average spin radius to be determined, and hence the moment of inertia theory to be applied.

Results for the high fuel level flight tests are summarised in Table 4 where the fuel mass is calculated based on $0.721kg/l$. The spin radius is calculated based on an average of the repeated spins in the same direction. The spin frequency has been found from averaging the results found by both the FFT method and the AHRS data. Hence, a 95% confidence interval has been calculated to take into account the equipment accuracy as discussed in Section IV. These initial results suggest that the aircraft has a tendency to spin

[a]An approximate flight path angle for the spin decent is found from analysing the on-board video

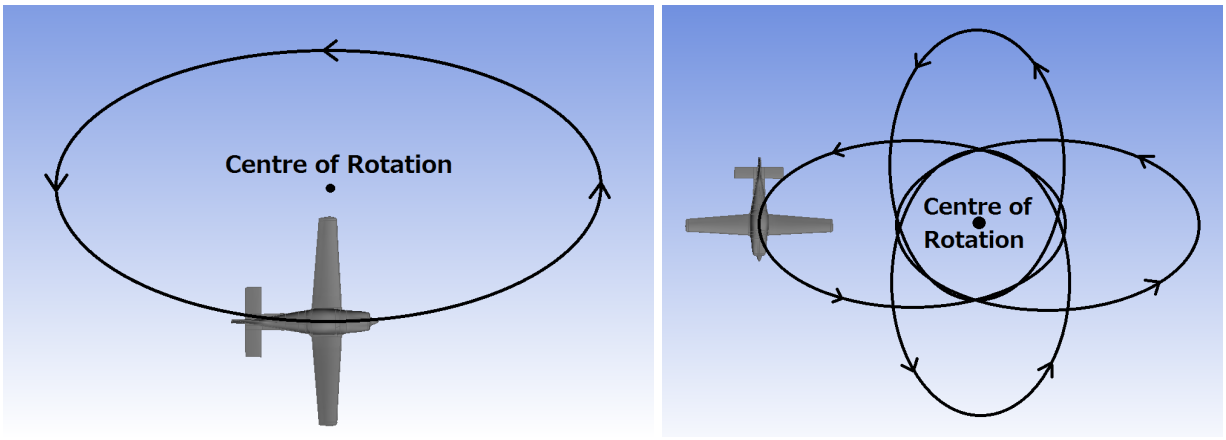

Figure 8. Diagram of an elliptical (left) and an epicycloidal (right) spin trajectory.

at a higher frequency to the right even though it tracks a larger spin radius. This is assumed to be in part due to the P-factor, but repeated flight tests with further spin demonstrations would be required, with fuel levels as close as possible for the left- and right-hand spins, to conclude this observation more decisively.

Spin Direction	Fuel Mass (kg)	Spin Radius (m)	Spin Freq (Hz)
Left-hand Spin	91.57	4.11	0.3087
Right-hand Spin	89.04	4.23	0.3141
95% CI		±0.065	±0.0039

Table 4. High fuel load spin trials.

VII. Low Fuel Load Spin Frequency Predictions and Comparison to Flight Test Data

The results for the high fuel load flight test may now be used in conjunction with the derivation in Section V to theoretically predict the change in spin frequency for a low fuel load flight test. If the mass of fuel on-board is known, the aircraft's dominant moments of inertia can be calculated to find a ratio of angular velocities, and hence spin frequencies for both cases. It is predicted that the change in fuel load will negligibly effect the spin frequency since the corresponding moment of inertia is dominated by larger ones, such as that from the engine mass.

In the following section, the dominant masses of the aircraft, for example the engine, will be treated as point masses acting in the centre of each individual part. The moments of inertia are therefore calculated based on the distances of the point masses relative to the C. G. of the aircraft, see Fig. (9). Information regarding the distances and masses are given in Table 5.

	Distance from C. G. (m)	Mass (kg)
Engine/Airframe/Pilots	0	250 + 505 + 150 = 905
Left Fuel Tank	-2.07	30 (low fuel), 65 (high fuel)
Right Fuel Tank	2.07	30 (low fuel), 65 (high fuel)
Total		965 (low fuel), 1035 (high fuel)

Table 5. Bulldog point mass locations with respect to the aircraft C. G. with approximate masses, see Fig. (9).

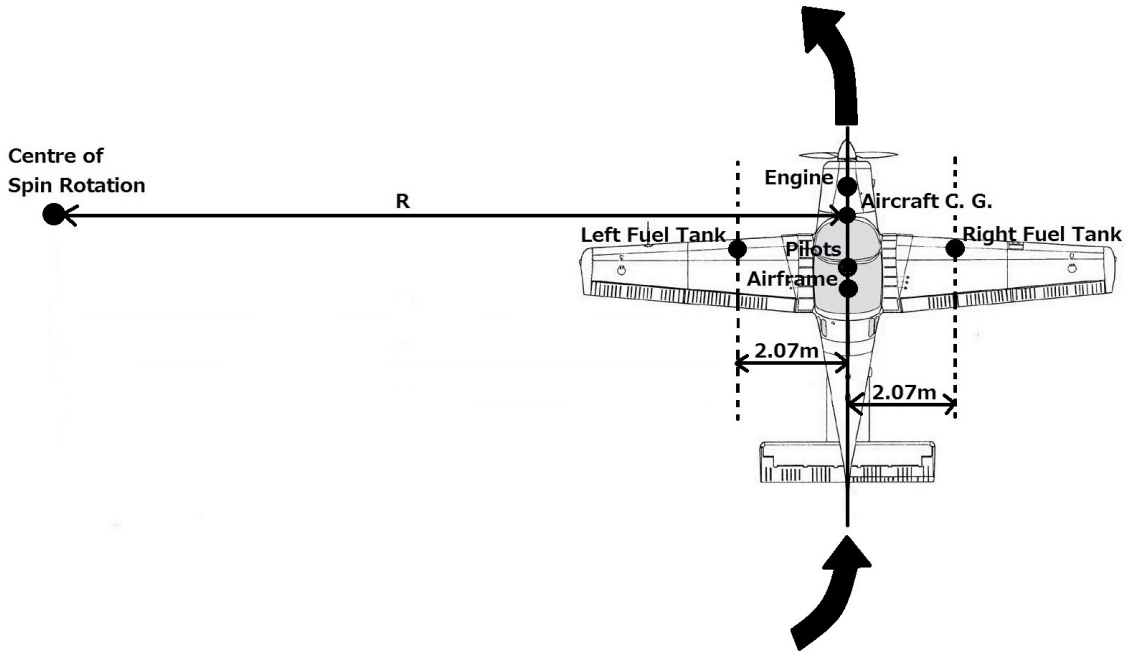

Figure 9. Diagram showing the relative distances (in the spin axis) of the considered point masses with respect to the C.G. location and the spin radius.

The procedure for calculating the moments of inertia for any given spin are as follows. Firstly, using the method described in the section above, the average spin radius for a left- and right-hand spin is determined. Then, the moments of inertia are calculated for each significant point mass using Fig. (9) and Table 5. So, firstly for a left-hand spin,

$$\begin{aligned} I_{Engine,Airframe,Pilots} &= mR^2 = 905 \times (4.11)^2 = 15287.35, \\ I_{LeftFuelTank} &= mR^2 = 45.79 \times (4.11 - 2.07)^2 = 190.56, \\ I_{RightFuelTank} &= mR^2 = 45.79 \times (4.11 + 2.07)^2 = 1748.83, \end{aligned}$$

and also for a right-hand spin,

$$\begin{aligned} I_{Engine,Airframe,Pilots} &= mR^2 = 905 \times (4.35)^2 = 17124.86, \\ I_{LeftFuelTank} &= mR^2 = 44.52 \times (4.35 - 2.07)^2 = 231.43, \\ I_{RightFuelTank} &= mR^2 = 44.52 \times (4.35 + 2.07)^2 = 1834.95, \end{aligned}$$

Therefore, the total moment of inertia for a high fuel load left-hand spin is 17226.74 kgm^2 and for a right-hand spin is 19191.25 kgm^2.

Since the fuel loads for the low fuel level flight tests are known, a theoretical prediction for the change in spin frequency can be calculated, assuming the same spin radii.

The moments of inertia, I, for the left-hand spin in the low fuel configuration is calculated as,

$$\begin{aligned} I_{LeftFuelTank} &= mR^2 = 24.16 \times (4.11 - 2.07)^2 = 100.54, \\ I_{RightFuelTank} &= mR^2 = 24.16 \times (4.11 + 2.07)^2 = 922.73, \end{aligned}$$

and for the right-hand spin,

$$\begin{aligned} I_{LeftFuelTank} &= mR^2 = 22.89 \times (4.35 - 2.07)^2 = 118.99, \\ I_{RightFuelTank} &= mR^2 = 22.89 \times (4.35 + 2.07)^2 = 943.44, \end{aligned}$$

Therefore, the total moment of inertia for a low fuel load left-hand spin is 16310.62 kgm^2 and for a right-hand spin is 18187.30 kgm^2. Then since,

$$I_{LowFuel}\Omega_{LowFuel} = I_{HighFuel}\Omega_{HighFuel}, \tag{6}$$

the ratio of angular velocity for the left-hand spin is 1.056 and for a right-hand spins is 1.055. Hence, by the conservation of angular momentum, the aircraft is predicted to spin to the left 5.6% faster in the low fuel configuration than in the high fuel configuration, and 5.5% faster to the right.

In terms of the observed spin frequency, if the aircraft spins to the left at 0.3087 Hz and to the right at 0.3141 Hz with the high fuel load, then it is predicted to spin to the left at 0.3260 Hz and to the right at 0.3314 Hz with the low fuel load. This theoretical prediction can be compared to the flight test data from the low fuel load trials.

The AHRS and FBGs data for the low fuel flight test is processed and analysed in the same way as in the high fuel flight test to calculate the frequency of a typical left- and right-hand spin. Fig. 10 shows a summary of the flight test results in comparison to the theoretical predictions. Calculations for hypothetical minimum and maximum fuel load cases are also included. Flight test results show that left-hand spins in the low fuel load configuration are 4.3% faster than in the high fuel load configuration, and right-hand spins are 4.1% faster. This compares to the theoretical prediction of 5.6% faster to the left and 5.5% faster to the right.

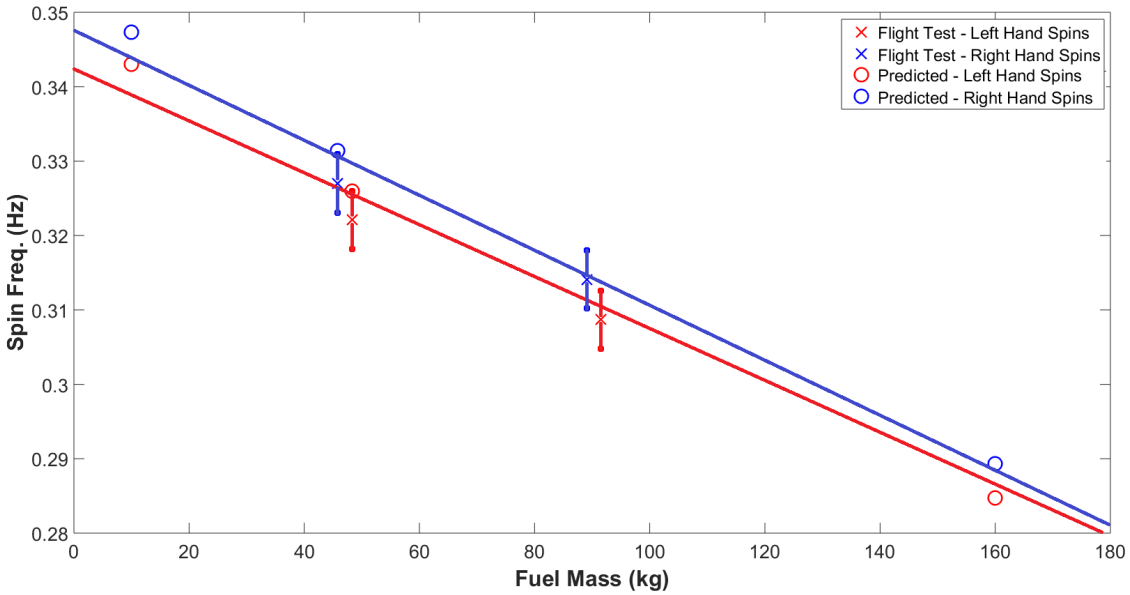

Figure 10. Summary of flight test data (with 95% confidence interval) and theoretical predictions on the effect of fuel load on the spin frequency.

It is seen from Fig. 10 that the theoretical approach predicts the spin frequencies to within the 95% confidence interval of the flight test results, however there is some overlap of the left- and right-hand spin intervals. Therefore, within the accuracy of the on-board equipment, the spin frequency alone would not be sufficient to determine the direction of the spin.

Despite this, the theoretical method is reliable in predicting whether the spin frequency will increase or decrease as a result of a higher or lower fuel load, and also the approximate magnitude of the change, on average to within 1% of the flight test results. The largest discrepancy between the theoretical predictions and the flight test data is for the right-hand spins, where the difference is approximately 1.5%. The theoretical model does not account for the P-factor and and hence could be the reason for this discrepancy. The P-factor is assumed to be the main reason for the general observation from Fig. 10 that right-hand spins are approximately 1.6% faster than left-hand spins.

Finally, the results shown in Fig. 10 suggest that the difference in spin frequency due to the fuel loading is negligible as predicted, even in the extreme hypothetical cases of maximum and minimum fuel loads.

In addition to the spin frequency analysis, the lateral g-force experienced by the pilot during a spin can also be calculated, see the summary of results given in Table 6. It is seen that the increase in spin frequency between the low and high fuel loads corresponds to a relatively insignificant increase in lateral g-force and hence is unlikely to be noticed by the pilot. A maximum difference of 0.77g is seen in the hypothetical extreme cases of minimum and maximum fuel loads.

Fuel Load (kg)	Theoretical Prediction or Flight Test Result	Direction of Spin	Spin Radius (m)	Spin Freq (Hz)	Lateral G-Force (m/s^2)
10.00	Predicted	Left	4.11	0.3430	1.95
10.00	Predicted	Right	4.35	0.3473	2.11
91.57	Flight Test	Left	4.11	0.3087	1.58
89.04	Flight Test	Right	4.35	0.3141	1.73
48.31	Predicted	Left	4.11	0.3260	1.76
45.78	Predicted	Right	4.35	0.3314	1.92
48.31	Flight Test	Left	4.11	0.3221	1.72
45.78	Flight Test	Right	4.35	0.3270	1.87
160.00	Predicted	Left	4.11	0.2847	1.34
160.00	Predicted	Right	4.35	0.2893	1.47
95% CI	Flight Test	Left	±0.065	±0.0039	±0.04
95% CI	Flight Test	Right	±0.065	±0.0039	±0.05

Table 6. Results Summary.

VIII. Conclusions and Discussion

The aim of this paper was to analyse the effect of the fuel load on a light aircraft spin. Research equipment fitted to a Scottish Aviation Bulldog allowed flight test data to be gathered for both high and low fuel load spins. This data was compared to results found via a theoretical approach derived from the classic literature.

Results show that, as predicted, the change in spin frequency is minimal since the moments of inertia corresponding to the fuel load are dominated by the much heavier masses which make up the aircraft, such as the engine. However, the increases in spin frequency for the low fuel load flight tests as compared to the high fuel load flight tests, of around 4-5%, were predicted to within the 95% confidence interval of the on-board equipment by the theoretical approach. It was also noted that for a given fuel load, a spin to the right is faster than to the left due to the yawing effect of the propeller. Furthermore, hypothetical maximum and minimum fuel load cases were analysed to show that the increase in lateral g-force experienced by the pilot is thought to be negligible.

Due to the uncertainties in the data, it is recommended that further flight tests should be conducted for a range of fuel levels aiming to obtain data for left- and right-hand spins when the fuel level is as equal as possible. Furthermore, if possible, an external video recording of example left- and right-hand spins from directly above or below the aircraft in flight, would aid validation of the findings in this paper.

References

[1]W. J. Duncan. *The Principles of the Control and Stability of Aircraft - 2nd Edition*. Cambridge University Press, United Kingdom, 1959.

[2]A. W. Babister. *Aircraft Stability and Control*. Pergamon Press, United Kingdom, 1st edition, 1961.

[3]B. Dikinson. *Aircraft Stability and Control for Pilots and Engineers*. Isaac Pitman and Sons Ltd London, 1968.

[4]F. S. Malvestuto, L. J. Gale, and J.H Wood. Compilation of test data on free spinning airplane models tested in the Langley 15-foot and 20-foot free-spinning tunnels. *NACA*, (L7E15), 1947.

[5]G. I. Rubio. Flight Testing of Different Sensors on a Bulldog Flight Test Aircraft. Master's thesis, Cranfield University, 2015.

[6]N. J. Lawson, N. Salmon, J. E. Gautrey, and R. Bailey. Comparison of flight test data with a computational fluid dynamics model of a Scottish Aviation Bulldog aircraft. *Aeronautical Journal*, 117:1273–1291, 2013.

[7]N. J. Lawson, R. Correia, S. W. James, M. Partridge, S. E. Staines, J. E. Gautrey, K. P. Garry, J. C. Holt, and R. P. Tatam. Development and application of optical fibre strain and pressure sensors for in-flight measurements. *Measurement Science Technology*, 27(10), 2016.

[8]N. Michel and A. Guinamard. Ig-500a sub-miniature AHRS user manual. *SBG Systems*, 2013.

[9]W. F. Phillips. *Mechanics of Flight*. John Wiley and Sons, Inc., 2010.

[10]ESDU. Fluid forces on non-streamline bodies - background notes and description of the flow phenomena. Technical Report 71012, UK, 1971.

[11]H. E. Taha, M. R. Hajj, and P. S. Beran. State-space representation of the unsteady aerodynamics of flapping flight. *Journal of Aerospace Science and Technology*, 34, 2014.

[12]B. Montgomerie. Drag coefficient distribution on a wing at 90 degrees to the wind. *Petten*, (ECN-C–95-061), 1996.

[13]S. F. Hoerner and Borst H.V. *Fluid Dynamic Lift*. Mrs. L. A. Hoerner, WA, USA, 2nd edition, 1985.